CrossMark

An Improved Empirical Harmonic Model of the Celestial Intermediate Pole Offsets from a Global VLBI Solution

Santiago Belda[1,2,4] ⓘ, Robert Heinkelmann[2], José M. Ferrándiz[1], Maria Karbon[2], Tobias Nilsson[2], and Harald Schuh[2,3]
[1] Department of Applied Mathematics, University of Alicante, Carretera San Vicente del Raspeig s/n,
San Vicente del Raspeig, E-03690 Alicante, Spain; Santiago.belda@ua.es
[2] Helmholtz Centre Potsdam, German Research Centre for Geosciences (GFZ), Telegrafenberg, A17, D-14473 Potsdam, Germany
[3] Institute of Geodesy and Geoinformation Science, Technical University of Berlin, Straße des 17, Juni 135, 10623 Berlin, Germany

Abstract

Very Long Baseline Interferometry (VLBI) is the only space geodetic technique capable of measuring all the Earth orientation parameters (EOP) accurately and simultaneously. Modeling the Earth's rotational motion in space within the stringent consistency goals of the Global Geodetic Observing System (GGOS) makes VLBI observations essential for constraining the rotation theories. However, the inaccuracy of early VLBI data and the outdated products could cause non-compliance with these goals. In this paper, we perform a global VLBI analysis of sessions with different processing settings to determine a new set of empirical corrections to the precession offsets and rates, and to the amplitudes of a wide set of terms included in the IAU 2006/2000A precession-nutation theory. We discuss the results in terms of consistency, systematic errors, and physics of the Earth. We find that the largest improvements w.r.t. the values from IAU 2006/2000A precession-nutation theory are associated with the longest periods (e.g., 18.6-yr nutation). A statistical analysis of the residuals shows that the provided corrections attain an error reduction at the level of 15 μas. Additionally, including a Free Core Nutation (FCN) model into a priori Celestial Pole Offsets (CPOs) provides the lowest Weighted Root Mean Square (WRMS) of residuals. We show that the CPO estimates are quite insensitive to TRF choice, but slightly sensitive to the a priori EOP and the inclusion of different VLBI sessions. Finally, the remaining residuals reveal two apparent retrograde signals with periods of nearly 2069 and 1034 days.

Key words: astrometry – catalogs – reference systems – techniques: interferometric

1. Introduction

Due to gravitational attractions from the Moon, Sun, and planets, the Earth rotation axis shows various periodical and irregular motions w.r.t. its figure axis and w.r.t. an ideal inertial reference system. The General Assemblies of the International Astronomical Union (IAU) held in 2000 and 2006 defined the transformation from the relevant Celestial Reference System (CRS) to the Terrestrial Reference System (TRS) with the help of the so-called Celestial Intermediate Reference Frame (CIRF), e.g., Urban & Seidelman ([2013](#)). The precession-nutation angles give the orientation of the CRF (usually the International Celestial Reference Frame, or ICRF) w.r.t. the CIRF. The position of the CIRF pole or Celestial Intermediate Pole (CIP) in the CRF is defined by the precession-nutation angles, the term precession being used when the long-term motion is referred to, and nutation being applied to faster, quasi-periodic variations with periods larger than two solar days in the CRF according to the IAU resolutions; see, e.g., the International Earth Rotation and Reference Systems Service (IERS) Conventions (2010; Petit & Luzum [2010](#)).

The transformation from CRS to TRS is completed through the three rotation angles that connect the CIRF to the used TRF, often designed as Earth rotation parameters (ERPs). Two

of them, x_p and y_p, give the relative position of the CIRF and TRF poles and constitute the so-called polar motion (PM) parameters, while the third one accounts for the irregular Earth diurnal rotation, usually expressed by the parameter dUT1, which is obtained from the difference between universal time UT1 and UTC (universal time coordinated). The ensemble of the two precession-nutation angles and the three ERPs is usually designated as Earth orientation parameters (EOPs). That is the terminology adopted in the IERS Conventions (2010) and followed in this paper.

The IAU2000A nutation (Mathews et al. [2002](#)) and IAU2006 precession models (Capitaine et al. [2003](#), [2005](#)) were adopted to provide accurate approximations and predictions of the CIP. However, they are not fully accurate and VLBI (Very Long Baseline Interferometry) observations show that the CIP deviates from the position resulting from the application of the IAU2006/2000A model (see e.g., Petit & Luzum [2010](#)). Those deviations or offsets of the CIP are known as Celestial Pole Offsets (CPOs) and are denoted as (dX, dY). Currently, accurate observations of CPO can only be obtained by the VLBI technique. The observed CPO can quantify the deficiencies of the IAU2006/2000A precession-nutation model, including the astronomically forced nutations and a component of nutation that is considered unpredictable. The latter is mainly constituted by the free core nutation (FCN), which is excited by angular momentum exchanges between the Earth's mantle and its fluid layers (Toomre [1974](#); Smith [1977](#); Wahr [1981](#)). It has a retrograde long-period of about 430 days (with average amplitudes of about 100 μas) relative to the inertial frame (Krásná et al. [2013](#)), or a period slightly shorter than 1 day in the retrograde-diurnal band, relative to the rotating terrestrial frame. The absence of a model for FCN prediction is what causes the uncertainty of the IAU

---

[4] Corresponding author address and email: Department of Applied Mathematics, University of Alicante, Carretera San Vicente del Raspeig s/n, San Vicente del Raspeig, E-03690 Alicante, Spain

2006/2000A precession-nutation model to be roughly of the order of 0.2 mas (Dehant et al. 2003). Due to the variable character of amplitudes and phases of the FCN effect, accurate empirical models based on VLBI estimates are required. Currently, different empirical FCN models, which were determined using different adjustment strategies (Lambert & Dehant 2007; Krásná et al. 2013; Malkin 2013a; Belda et al. 2016), are available. The IERS Conventions recommend the model of Lambert (2007), which was obtained by fitting the FCN amplitude on a 2-year interval running by steps of one year.

Free inner core nutation (FICN) is one of the four free rotational modes of the Earth considered in the theory of Earth rotation, corresponding to the mode designated prograde free core nutation (PFCN) in Mathews et al. (1991). Detecting this signal in the observational data is a very important scientific task that would allow for substantial improvement of the knowledge about the Earth's interior and dynamics (Malkin 2013b). Consequently, it could bring us significantly closer to meeting the accuracy goals pursued by the Global Geodetic Observing System (GGOS) of the International Association of Geodesy (IAG), i.e., 1 mm accuracy and 0.1 mm/year stability on global scales in terms of the ITRF defining parameters (Plag & Pearlman 2009). Mathews et al. (2002) were the first to discuss the existence of this resonance in VLBI observations at a period of approximately 1035 days supposedly caused by the FICN. According to Dehant et al. (2005), the dynamics of the atmosphere and the oceans could excite the FICN to amplitudes of a few tens of microarcseconds (μas).

Since the adoption of IAU2000, VLBI observations have more than doubled in number and the quality of the data has significantly improved. Empirically speaking, we assume that evaluating the consistency and updating the precession-nutation model could provide the necessary accuracy for detecting signals of the aforementioned order of magnitude. These issues were discussed by the past and more recent studies done by Charlot et al. (1995) and Gattano et al. (2017), respectively. In the former study, the IAU 1980 nutation theory (Seidelmann 1982) was evaluated on the basis of combining VLBI and Lunar Laser Ranging (LLR) data analyses, whereas in the latter study different nutation series determined by different VLBI Analysis Centers (AC) of the International VLBI Service for Geodesy and Astrometry (IVS; Nothnagel et al. 2015) were compared.

It is common practice in geodetic VLBI analysis to distinguish between the so-called arc parameters and global parameters. This terminology reflects the time epochs for which the parameters are valid. Arc parameters are parameters that are valid only during a particular observation session or parts of it. These are, for example, the clock parameters, zenith wet delay, or tropospheric gradients which customarily vary on a sub-daily basis, whereas global parameters are valid for longer time periods and not only for a single observing session. For example, radio source coordinates, relativistic parameters, and station coordinates and velocities can belong to the latter category of parameters. The so-called global analysis uses a large number of VLBI sessions and allows for solving for both arc and global parameters. The computational strategy is based on a separation of the normal equation (NEQ) system into two parts. The first part contains the parameters that are estimated and constitute the relevant output for a certain planned analysis. And the second part corresponds to the remaining parameters,

which are "reduced" from the equations. Note that those "reduced" parameters still belong to the functional model of unknown parameters and are estimated implicitly from the session-wise NEQ during the least-squares adjustment. One possible approach is to accumulate reduced NEQ from single sessions that no longer contain arc parameters, and then to solve for the global parameters. Then, the arc parameters for each session can be determined in a second step by substituting the estimated global parameters (Haas 2004).

In this paper, we empirically evaluate the consistency, systematics, and deviations of the IAU 2006/2000A precession-nutation model using several CPO time series derived from the global analysis of VLBI sessions starting in 1990. To reflect the impact of frames and other processing strategies on the CPO estimates, we alternate several analysis settings (Section 2). In Section 3, the various series are then used to readjust the precession offset and rate, as well as the main nutation amplitudes available in the IAU 2006/2000A precession-nutation model for the sake of empirically improving the conventional values adopted by the IAU and the IAG as published in the IERS Conventions (2010). The empirical FCN model (Belda et al. 2016) is also included in the adjustment, after a comparison with other empirical FCN models. In Section 4, the remaining residuals of the fit are analyzed and discussed by investigating possible geophysical signals in the frequency band where the FICN is expected. Finally, concluding remarks are given in Section 5.

2. Methodology

2.1. Global VLBI Solution

The reassessment of the precession and nutation terms in analogy to the IAU 2006/2000A precession-nutation model is empirically done by performing different VLBI data analyses with the GFZ version (Nilsson et al. 2015) of the Vienna VLBI Software (VieVS) (Böhm et al. 2012). As detailed in Section 2.2, we apply several VLBI processing options. In order to achieve a high degree of consistency between the VLBI data (and implicitly in the CPO estimates) with respect to the ICRF2, we mainly focus on analyzing VLBI data globally, processed at once in an accumulated normal equation system. The number of sessions amounts to 2990, ranging from 1990 to 2010. We decided to exclude the sessions before 1990 and after 2010.0 because of the inaccuracy of VLBI data in the early years (Malkin 2013a) and because the ICRF2 is based on VLBI data until 2009 March only. The single-session analysis was based on the IERS Conventions (2010). Before the global solution/adjustment, we discarded VLBI sessions with a posteriori sigmas of unit weights larger than 3. In addition, sources observed less than 15 times over 2 years, which appear in less than 3 VLBI sessions, and the coordinates of the so-called ICRF2 special handling sources, were reduced in order to refine the CPO measurements. Consequently, a total of 677 radio sources were estimated. The radio source velocities were fixed to zero (no proper motion allowed), whereas station positions along with the ERP (x_p, y_p, dUT1) were reduced from the NEQ-system (in the sense explained in Section 1). Additionally, the datum definition of the TRF was constrained by applying no-net-translation (NNT) and no-net-rotation (NNR) conditions at the session level, referring to the station coordinates reported in the respective catalogs. Although CPOs are usually determined as arc parameters from single VLBI

Table 1
Overview of the Different Applied Approaches (A and B)

			Choice of the a Priori Data	
TRF	EOP Series	EOP	ERP and IAU2006/2000A	ERP and IAU2006/2000A + FCN B16
ITRF2014	USNO finals	A1.a and B1	A2.a	A3.a
	IERS 08 C04	A1.b	A2.b	A3.b
VTRF2008	USNO finals	B2	⋯	⋯
ITRF2008	USNO finals	B3	⋯	⋯

sessions, in our approach the CPOs and source coordinates were estimated as global parameters by imposing no-net-rotation conditions with respect to the ICRF2 defining sources (Fey et al. 2015). We had two motives. First, the comparison/update of precession-nutation model terms is expected to gain consistency and accuracy when using a global solution, since determining those parameters from individual VLBI sessions would add additional noise, e.g., rotation of sub-frames or other datum inconsistencies (Belda et al. 2017). Second, global parameters allow direct calculation of formal errors, whereas the time series only allow for an empirical step-wise error assessment. Finally, we repeated the VLBI analysis when extending the period until 2015.0, with a total of 3594 sessions, to study the impact of including the most recent data. In this case, 744 radio sources were included in the solutions.

2.2. General Design of the Different Testing Approaches

In an ideal case, the estimated values of the CPO should be the same, independent of the a priori values. However, highly accurate estimation of the full set of EOP is not simple from either a mathematical or physical perspective, and the possibility of having effects derived from the choice of the initial solution should not be discarded (Belda et al. 2017). Following up on this basic idea, multiple VLBI analyses were carried out with different a priori EOP series (IERS 08 C04 (Bizouard & Gambis 2009), United States Naval Observatory (USNO) finals), and TRFs (ITRF2014 (Altamimi et al. 2016), ITRF2008 (Altamimi et al. 2011), VTRF2008 (Böckmann et al. 2010)) to determine the effect of changing those inputs on the CPO, the precession constant and rate, and the main nutation terms of the 2006/2000A precession-nutation model. The former and latter approaches, designated "A" or "B" respectively in Table 1, are explained in the next paragraphs.

2.2.1. Test A: Different a Priori EOP Series

Using ITRF2014 and ICRF2, several global VLBI solutions were estimated from various a priori EOP series (USNO finals and IERS 08 C04) and different settings. In all cases, we performed a global analysis of all the VLBI data in the selected period of time that treats all the sessions jointly, to derive a series of differences dX, dY, between the X_{VLBI}, Y_{VLBI}, coordinates of the CIP estimated from VLBI data minus the a priori EOP values that define the case.

1. *Case A1.* A priori EOP values are taken from USNO finals (case A1.a) or IERS 08 C04 (case A1.b):

$$X_{\text{VLBI}} = (X_{\text{IERS/USNO}})_{\text{apriori}} + dX$$
$$Y_{\text{VLBI}} = (Y_{\text{IERS/USNO}})_{\text{apriori}} + dY. \quad (1)$$
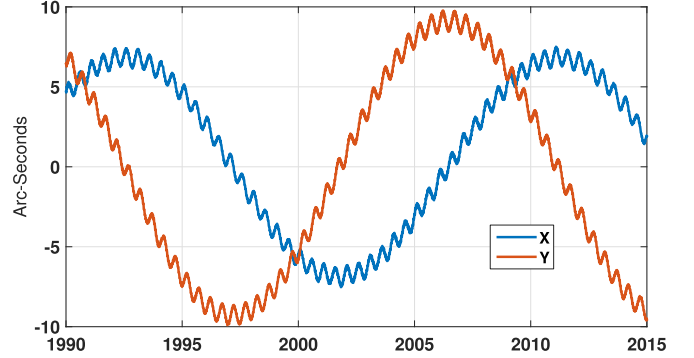

Figure 1. Celestial Pole Coordinates estimated from case A1.a using USNO finals as a priori values. Precession and obliquity rates were removed between 1990 and 2015.

This case serves to compare the new global solution to well-known local solutions such as the conventional IERS C04 and USNO finals.

2. *Case A2.* A priori EOP values are: (1) the X, Y, predicted by the IAU2006/2000A model:

$$X_{\text{VLBI}} = (X_{\text{IAU2006/2000A}})_{\text{apriori}} + dX$$
$$Y_{\text{VLBI}} = (Y_{\text{IAU2006/2000A}})_{\text{apriori}} + dY; \quad (2)$$

and (2) the ERP from USNO finals in A2.a and from IERS 08 C04 in A2.b. This choice is similar to Belda et al. (2016). This case is the closest to compare the new global solution to the conventional definition of CPO, based on IAU2000A.

3. *Case A3.* A priori EOP values are: (1) the sum of the X, Y, predicted by the IAU2006/2000A model and the free nutation provided by one of the empirical *FCN* models by Belda et al. (2016; hereafter B16) either derived from USNO finals (case A3.a) or from IERS 08 C04 (case A3.b):

$$X_{\text{VLBI}} = (X_{\text{IAU2006/2000A}} + X_{\text{FCN}})_{\text{apriori}} + dX$$
$$Y_{\text{VLBI}} = (Y_{\text{IAU2006/2000A}} + Y_{\text{FCN}})_{\text{apriori}} + dY; \quad (3)$$

and (2) ERP like in Case A2. This approach is useful for assessing the joint predictive capability of the a priori combined model, regarding the global solution as target.

For each of the aforementioned cases, the Celestial Pole Coordinates (CPCs, X_{VLBI} and Y_{VLBI}) were calculated using the adjustments obtained by VLBI (dX, dY). As an example, Figure 1 represents the CPCs of case A1.a using USNO finals as a priori values.

That test can provide an indication of the predicting capabilities of each a priori CPC series: the more accurate a starting EOP set is, the less variability the CPO has. Note that only the dX, dY resulting from case A2 can be strictly
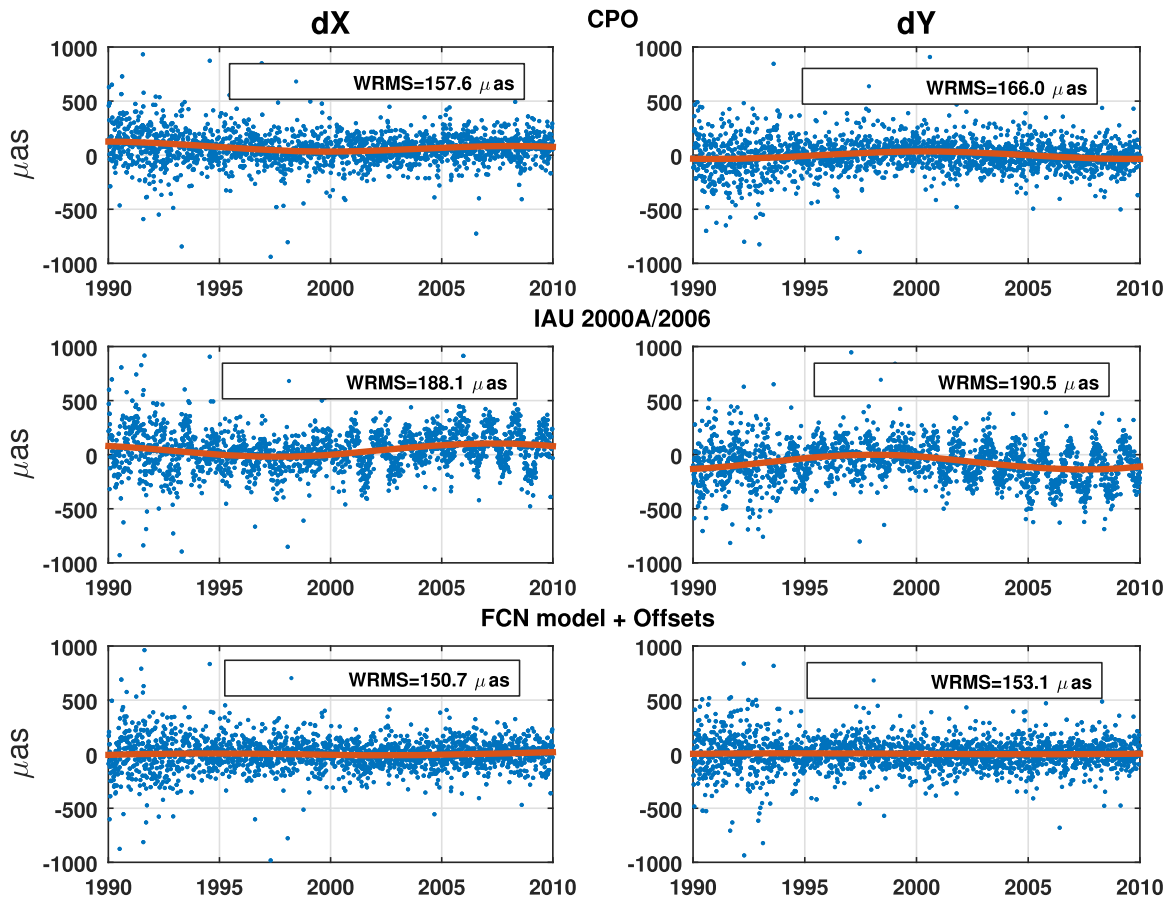
Figure 2. Adjustments to three CPO modeling approaches (blue dots). Top: case A1.a; middle: case A2.a; bottom: case A3.a. A priori data: USNO finals and ITRF2014. Left: *dX*. Right: *dY*. Orange line: 18.6-yr periodic term.

denominated as a CPO according to IAU resolutions, whereas the *dX*, *dY*, from cases A1 and A3 are more properly denoted as CPO-like parameters. However, for the sake of concision we denote of all them as CPO from now onward, taking into account the fact that the dispersion of each parameter provides an indication of the accuracy of its prediction by means of the assumed a priori solution. One remarkable feature is that case A3 produces the lowest WRMS for both coordinates (150.7 μas in *X* and 153.1 μas in *Y* as displayed in Figure 2, bottom), although one could reasonably expect that A1 would cause a priori values closer to our global VLBI solution, since both series (from IERS and USNO solutions) contain actual CPOs derived from a combination of VLBI observations.

If we compare the CPO adjustments (*dX*, *dY*) computed from cases A1 and A2 (Figure 2) we clearly find that a low-frequency part of about 18.6 yr of periodicity remains with approximately the same magnitude and opposite signs for *dX* and *dY*, respectively. Other authors already observed this signal and applied several methods to delete the small curvature, e.g., Capitaine et al. (2009) fitted a parabola plus a term of 18.6 year periodicity to the CPO adjustments. In case A3 this curvature is not visible in the adjustments resulting from the consideration of the FCN model fitted a priori, where the authors, in addition to accounting for the FCN signal, also accounted for such low-frequency signals in order to avoid contamination of the FCN signal determination (Belda et al. 2016).

To better compare the pairs of time series of CPO estimates, we calculated the weighted mean (WM) of the differences and the weighted root mean square (WRMS) differences between

each pair of them by means of the equation provided by Belda et al. (2017). In case A1.a, formal errors of *dX* range in the interval [7.5, 169.2] μas with a median of 60.7 μas; for *dY* the figures are similar, with a range [7.6, 169.6] μas and a median of 60.8 μas. There are no significant differences to the other cases. The orders of magnitude of the WM between all the cases are similar at about up to 2 μas, which is well below the current accuracy of the CRF axes at the level of 10 μas, providing evidence of the high consistency level of VLBI. This can be seen in Figure 3 (top and middle of the panel). However, it is important to note that the choice of a priori values (cases A1, A2, and A3) generates a noticeable scatter of about 50 μas and 70 μas from the USNO finals and IERS 08 C04, respectively. On the other hand, the smallest WRMS differences (around 10 μas) can be found when comparing case A2 to case A3. Moreover, note that case A1.a w.r.t case A1.b exhibits a WRMS difference of about 70 μas for both CPO components.

2.2.2. Test B: Different a Priori TRFs

This test is similar to case A1 but now CPOs were estimated making use of different terrestrial reference frames, i.e., B1: ITRF2014, B2: VTRF2008, and B3: ITRF2008 (Table 1), with USNO finals as a priori EOP values. It can assess the extent of the effect of the mutual consistency of EOP solutions and TRFs, indicated by the "repeatability" in terms of scatter or WRMS.
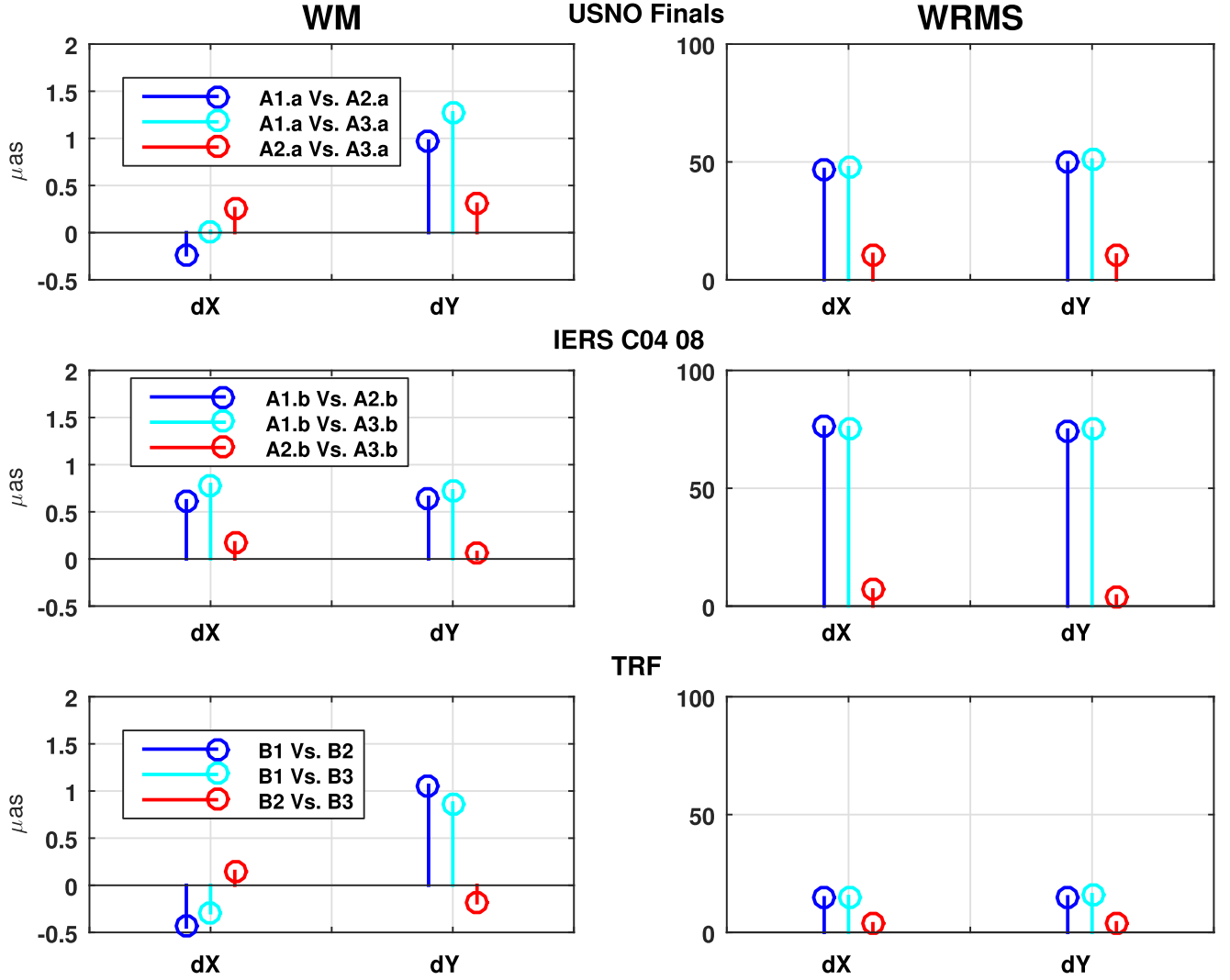
Figure 3. WM (left) and WRMS (right) differences between the EOP estimated with different a priori EOPs and different TRFs (legend: see Table 1). Units: μas. For an explanation of the various approaches see Table 1 and the text.

Once again, a low-frequency signal with a period of about 18.6 yr remains in the adjustments, with an amplitude comparable to the A1.a and A1.b approaches. CPO adjustments from cases B2 and B3 show practically identical scatter (of about 152 μas and 164 μas for X and Y, respectively). However, CPO estimates from ITRF2014 (case B1) produce a slight deterioration of the accuracy (157.6 μas in X and 166 μas in Y). The CPO differences between pairs of the different approaches (B1, B2, B3) are close to each other (Figure 4), showing only small WM ($<1.1 \mu$as) and WRMS differences (Figure 3, bottom). ITRF2008 w.r.t. VTRF2008 presents the smallest WRMS, about 5 μas, which was expected due to their mutual consistency: VTRF2008 presents the VLBI input to ITRF2008. On the other hand, ITRF2008 and VTRF2008 w.r.t ITRF2014 exhibit a scatter three times larger, which may be attributable to consistency issues w.r.t. the a priori EOP values and the different time spans of input data.

3. Least-squares Adjustment: Toward Refining the IAU 2006/2000A Precession-Nutation Models

The refinement of the VLBI-derived amplitudes of nutation terms presents a number of difficulties. Since some of the astronomical nutations have periods sufficiently close to the FCN, their amplitudes can be magnified by resonance. The most notable example is the retrograde annual nutation. On occasion, separation of periods is problematic and some periods need to be constrained to their theoretical amplitude values to properly fit the nutation series parameters—e.g., Herring et al. (2002) fixed the out-of-phase 386.0-day period amplitude to the MBH2000 a priori value.

In this study, to reduce the inconveniences derived from the aforementioned resonance effect, a preliminary FCN signal was subtracted from the CPC before fitting them to the main nutation amplitudes. The preliminary model was estimated from the CPO adjustments observed by VLBI w.r.t. the IAU 2006/2000A precession/nutation theory (the CIP coordinates) and following the sliding window length of 400 days' approach as outlined in Belda et al. (2016). The equations used to estimate the FCN model are:

$$X_{\text{FCN}} = A_c \cos(\sigma_{\text{FCN}}t) - A_s \sin(\sigma_{\text{FCN}}t) + X_0$$
$$Y_{\text{FCN}} = A_s \cos(\sigma_{\text{FCN}}t) + A_c \sin(\sigma_{\text{FCN}}t) + Y_0, \qquad (4)$$

where $\sigma_{\text{FCN}} = 2\pi/P$ is the frequency of FCN in the Celestial Reference System (CRS), A_C and A_S denote the amplitudes as
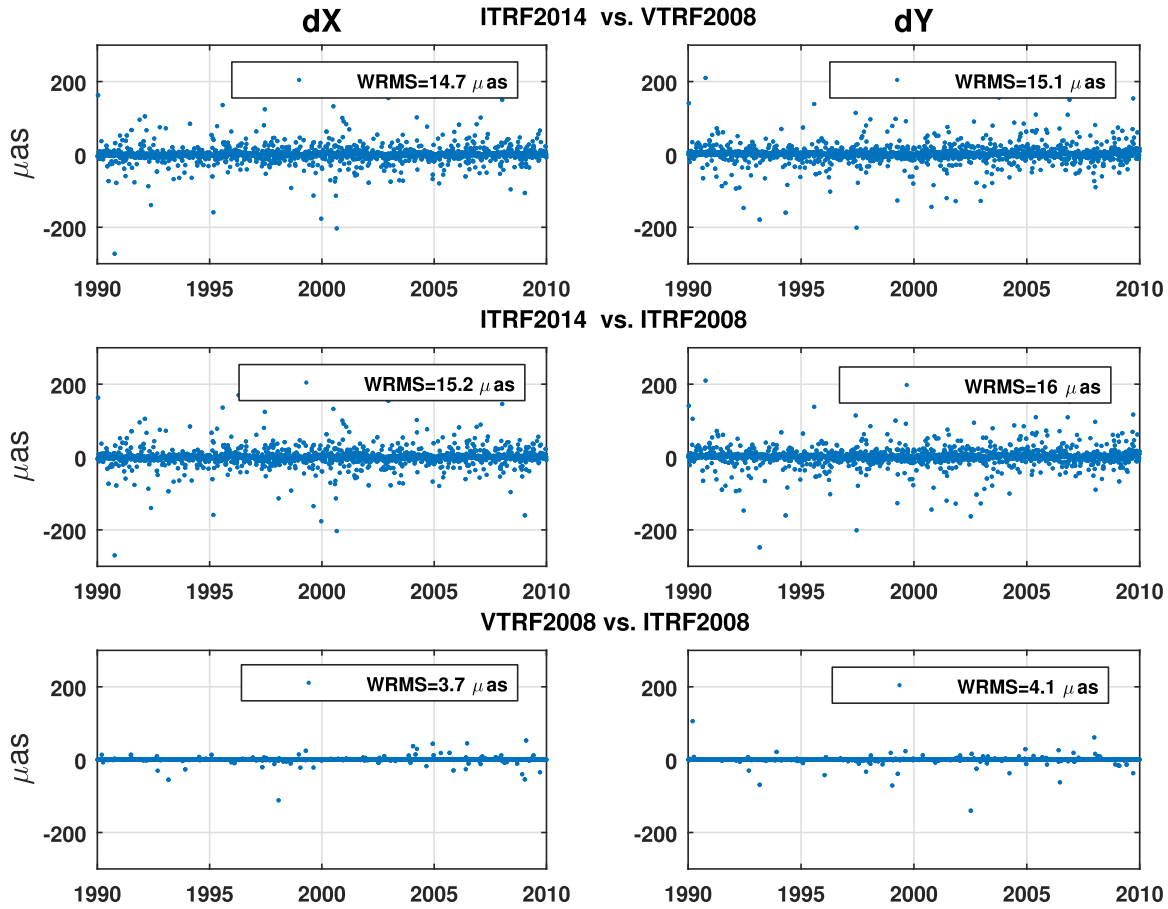
Figure 4. CPO differences (μas) between CPOs estimated with different TRFs: ITRF2014, ITRF2008, and VTRF2008. A priori EOPs are from USNO finals. Left: *dX*. Right: *dY*.

Table 2
Reassessment of Precession Offset b and Rate p

| Data Period | A Priori Values | | $b_x \pm \sigma$ | $b_y \pm \sigma$ | $p_x \pm \sigma$ | $p_y \pm \sigma$ | Before Fitting FCN[a] | | After Fitting FCN[a] | |
	TRF	EOP					r_x	r_y	r_x	r_y
1990–2010	ITRF2014	USNO finals								
		CPO	38.8 ± 2.1	-67.9 ± 2.1	1.4 ± 48.6	-144.2 ± 49.2	180.7	188.6	147.6	158.4
		IAU 2006/2000A	40.9 ± 1.8	-71.8 ± 1.9	2.9 ± 42.9	-83.1 ± 43.4	173.5	173.4	139.7	140.2
		IAU 2006/2000A + FCN	40.7 ± 1.8	-71.8 ± 1.9	-0.2 ± 42.7	-87.8 ± 43.1	172.4	173.0	138.5	140.0
	ITRF2014	IERS 08 C04								
		CPO	39.5 ± 2.3	-70.2 ± 2.3	-66.6 ± 53.9	-167.5 ± 54.5	193.7	194.9	163.7	166.7
		IAU 2006/2000A	40.5 ± 1.8	-71.9 ± 1.8	8.7 ± 42.6	-86.9 ± 43.0	173.1	173.0	139.1	140.3
		IAU 2006/2000A + FCN	40.5 ± 1.8	-72.0 ± 1.8	9.0 ± 42.4	-87.4 ± 42.9	173.1	172.9	139.0	140.2
	ITRF2008	USNO finals								
	ITRF2008	CPO	39.5 ± 2.1	-69.1 ± 2.1	-11.5 ± 47.9	-124.1 ± 48.5	177.4	187.0	144.1	156.6
	VTRF2008	CPO	39.6 ± 2.1	-68.9 ± 2.1	-10.8 ± 48.0	-128.8 ± 48.5	177.9	187.3	144.7	156.7
1990–2015	ITRF2014	USNO finals								
		CPO	38.6 ± 2.1	-68.9 ± 2.1	178.1 ± 27.1	-208.3 ± 27.3	187.9	194.0	144.2	154.0
		IAU 2006/2000A	41.0 ± 1.9	-73.2 ± 1.9	162.0 ± 24.0	-177.6 ± 24.2	184.9	183.2	138.6	140.1

Note. Formal errors for each parameter are provided following the $\pm$ sign. Units: μas or μas/century.
[a] Root mean squares *r* of the residuals after fitting the amplitudes of the main nutation terms of the IAU 2006/2000A precession-nutation model when considering or not considering the FCN effect through the estimated empirical models.

Table 3
Main Corrections to the IAU2000A Nutation Amplitudes

Period (days)	CPO	Median		Range		Median Error	
		As	Ac	As	Ac	As	Ac
6798.383	dX	−6.7	63.7	2.0	10.4	2.9	3.7
	dY	20.8	−63.0	4.3	6.3	2.9	3.7
3399.192	dX	−7.1	5.6	2.1	1.0	3.0	2.8
	dY	−6.3	−11.4	4.6	2.6	3.0	2.8
1615.748	dX	−1.4	−6.8	3.4	1.7	2.7	2.8
	dY	4.0	−8.7	3.5	2.9	2.7	2.8
1305.479	dX	0.1	5.6	1.5	1.4	2.8	2.8
	dY	7.2	12.2	1.6	1.1	2.8	2.8
1095.175	dX	2.7	−15.1	3.0	0.6	2.7	2.8
	dY	9.3	2.1	2.5	1.8	2.7	2.8
182.621	dX	10.6	−12.7	4.3	5.5	2.7	2.8
	dY	24.6	10.2	1.6	2.9	2.7	2.8
169.002	dX	8.6	0.4	3.3	2.3	2.7	2.7
	dY	4.2	4.6	5.0	2.5	2.7	2.7
29.531	dX	4.0	−0.3	4.2	2.7	2.8	2.8
	dY	6.4	8.7	4.2	1.8	2.8	2.8
27.555	dX	−3.5	−16.4	3.0	3.6	2.7	2.7
	dY	10.3	−5.9	6.1	4.7	2.7	2.7
27.093	dX	3.2	−6.0	3.0	2.0	2.7	2.7
	dY	3.9	11.9	3.4	1.9	2.7	2.7
26.985	dX	−3.1	4.3	1.9	3.3	2.8	2.8
	dY	1.9	−9.9	4.2	5.4	2.8	2.8
25.325	dX	−2.1	−2.9	3.2	1.6	2.7	2.8
	dY	8.3	−0.4	2.9	2.8	2.7	2.8
13.749	dX	1.6	3.0	3.0	2.2	2.6	2.7
	dY	0.4	9.2	4.6	1.2	2.6	2.7
13.661	dX	−22.4	−12.2	12.7	3.8	2.7	2.7
	dY	−0.9	5.9	7.2	6.7	2.7	2.7

Note. Corrections are estimated from the different VLBI global solutions (see Table 1) and feature the median amplitude, range and the median of the formal errors for each term. As and Ac correspond to sine and cosine components, respectively. Units: μas.

represented in the two components, t is the time relative to J2000.0, P is the FCN period, and X_0 and Y_0 are offsets. The amplitudes and offsets were estimated for each fitting interval. The offsets absorb the low-frequency part of the residual signal. Therefore, the contribution of the FCN to the CIP offsets (CPO) was computed using Equation (4) after removing the offsets X_0 and Y_0—which are thus ignored.

The estimated CPCs, which should now be almost free of the FCN signal, were used to recalculate and model the precession offset and rate, as well as the main nutation amplitudes corresponding to the periods included in the IAU 2006/2000A precession-nutation model. Our fitting method is based on the least-squares (LS) method, with weights taken as the inverse of the squared errors given by the VLBI estimates (e.g., Gattano et al. 2017). After LS fitting, the preliminary FCN model was added back to the remaining residuals in order to recalculate a final empirical FCN model using the same method as before.

3.1. Corrections to the Precession Offset and Rate Obtained by Various Approaches

Table 2 displays the corrections to the precession offsets and rates resulting from the LS adjustments. First, note that the order of magnitude of the correction to the precession offset is similar for all the approaches, which shows that this parameter

is not sensitive to the a priori values. The corrections w.r.t. the IAU 2006/2000A precession-nutation model show mean values close to 40 μas and −70 μas for b_x and b_y, respectively, with formal errors of about 2 μas. And second, the precession rates exhibit significantly different values depending on the approach, especially when compared to case A1, i.e., the a priori CPOs taken from IERS 08 C04 or USNO finals. Note that the precession rate p_y, which corresponds to the obliquity rate, presents the largest deviations (differences near 70 μas/century—small effect), with formal errors of 50 μas/century for both components (p_x and p_y). The magnitudes of these errors are completely in accordance with Liu & Capitaine (2017) and Gattano et al. (2017).

The inclusion of our FCN model into a priori CPO coordinates (approach A3) provides the smallest residuals (rms of 138.5. μas in dX and 140.0 μas in dY after removing the FCN oscillations). In addition, it causes an rms reduction of about 15 μas w.r.t. case A1. Analyzing the different TRFs, the most comparable results are reached between ITRF2008 and VTRF2008 (approaches B2 and B3) since they are the most consistent with ICRF2—at least regarding the years of data used in their realization. On the other hand, the poorest accuracy (rms) was found with ITRF2014 and USNO finals or IERS 08 C04 as a priori EOPs, mainly because these EOP series are not consistent with this frame. Note that the inclusion of additional more recent VLBI data up to 2015.0 causes a significant reduction of the formal error in precession rates, of about 50%. However, the estimated rates using different time spans (1990–2015 versus 1990–2010) show significant differences of about 170 μas/cy and 100 μas/cy for p_x and p_y, respectively.

3.2. Corrections to the Main Nutation Amplitudes

In this section, we use our previous global VLBI solutions to fit a set of corrections to the amplitudes given in IAU2000A. That theory was fitted to observations in 2000 using only 21 terms (Herring et al. 2002) and their WRMS were noticeably larger than the WRMS attainable at present. We start from a set of 197 terms that correspond to the lunisolar nutations with amplitudes larger than 4 μas, and are hence smaller than the set used by Petrov (2007) for fitting an empirical harmonic model for the Earth's three Euler angles. When two close frequencies do not meet the separation criterion, the frequency with larger amplitude in IAU2000 was kept and the other one was removed from the fitting. The criterion is the standard one, which was successfully applied by Petrov before: the frequency separation was considered unfeasible when the difference was smaller than $2\pi/\Delta T$, where ΔT denotes the interval length of observations, here 20 years; the resulting difference in frequencies is less than $\approx 10^{-8}$ rad s^{-1}. In this way, the total number of constituents used in the fit was reduced to 178. The corrections to the remaining amplitudes were derived for each of the global solutions described in the previous sections, together with their formal errors that stayed below 3 μas—all but the one for the 18.6-yr period.

Table 3 contains a summary of the most significant amplitude deviations, ordered by decreasing absolute values of the period. Only the terms with amplitude corrections larger than three times the median error are displayed, using a row for each CPO. The arguments for each period are the same that appeared in IAU2000A and are thus not displayed for the sake of concision. Columns headed by As and Ac show the
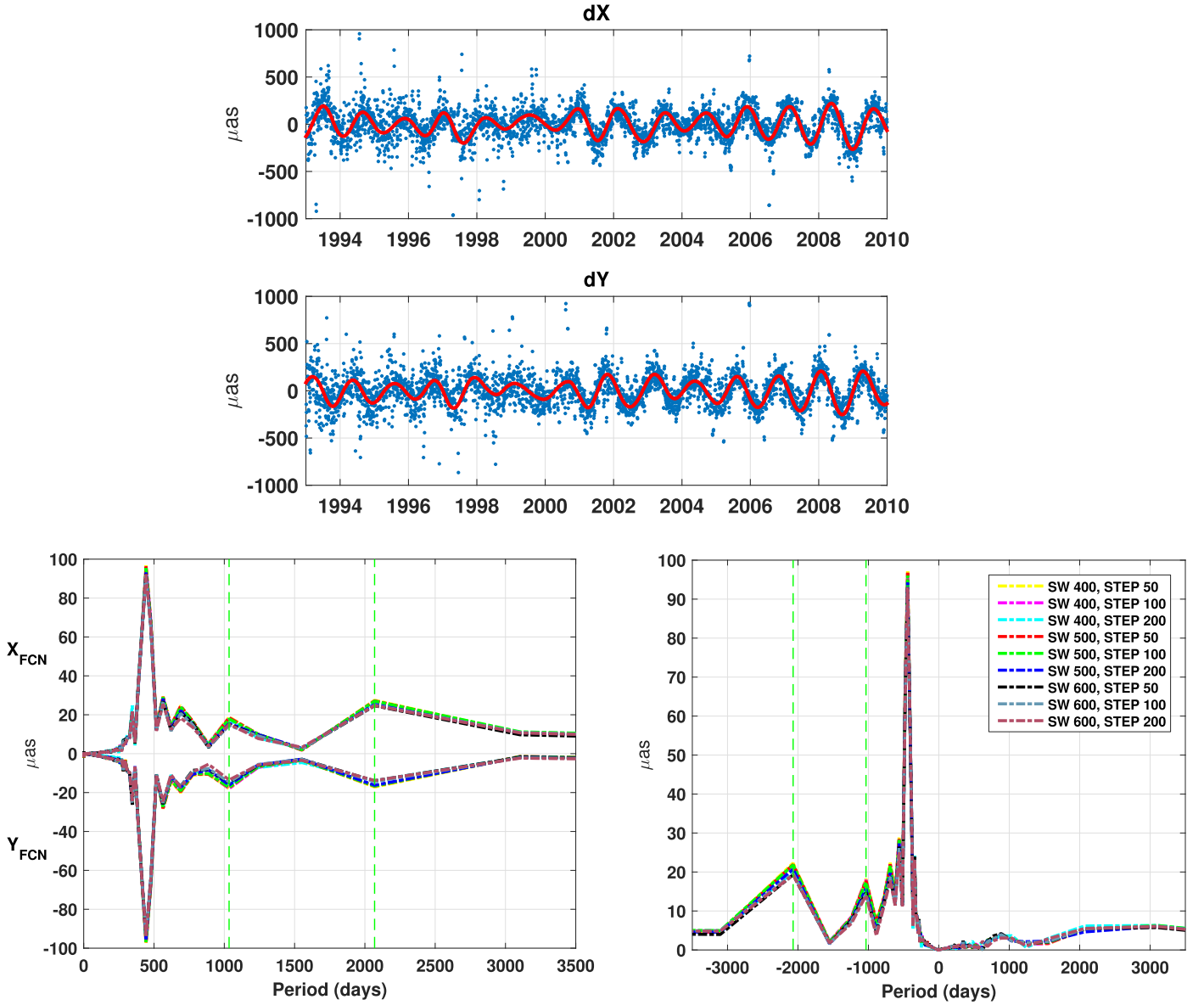
Figure 5. Upper plot: CPOs (blue dots) and FCN model (red line). Lower plots: Fourier spectra estimated from X_{FCN} and Y_{FCN} (left) and $X_{FCN} + i\,Y_{FCN}$ (right) using different window lengths and different step sizes between subsequent fits.

corrections to the amplitudes of the sine and cosine terms for the relevant argument, respectively. The values given in the table are obtained as the median of the corresponding corrections provided by each of the different approaches. Table 3 also displays the range of amplitude corrections (i.e., the maximum difference between the maximum and minimum values for all the solutions) and the median of the formal errors. The comparison of both parameters is useful to get more insight into the magnitude of the actual errors and repeatability. Mainly, the most significant deviations occur at the longest periods, particularly the 18.6-yr nutation.

4. Detailed Study of the Remaining Residuals

After the estimation of the selected set of nutation amplitudes, including the free motion associated with the FCN, a detailed study of the remaining residuals is presented. To ensure the "cleanness" of the residual time series we discarded the rather noisy data before 1993—a fact also pointed

out by Chao & Hsieh (2015). Consequently, our study is solely based on post-1993 data, for better quality. Figure 5 displays the FCN model that was calculated with a sliding window length of 400 days and a step size of 50 days using a priori CPOs from USNO finals (approach A1.a), along with the Fourier spectra estimated from X_{FCN} and Y_{FCN} (Equation (4)), and the complex quantity $X_{FCN} + i\,Y_{FCN}$. The FCN signal, with its dominant retrograde period that is somewhat longer than a year, is well captured across the Fourier spectra. Note that some more long-periodic signals appear in the retrograde nutation frequency band (Figure 5 bottom right); we will investigate these below.

In the time series of the parameters named X_0 and Y_0 in Equation (4), estimated together with the FCN corrections, which absorb the low-frequency signals and suppress the high-frequency signals, we clearly detect two long-periodic oscillations by means of Fourier analysis performed independently for both the real variables X_0 and Y_0 and the complex notation $X_0 + i\,Y_0$ (Figure 6). First, a clear signal at about 2069 days (≈ 5.7 years)
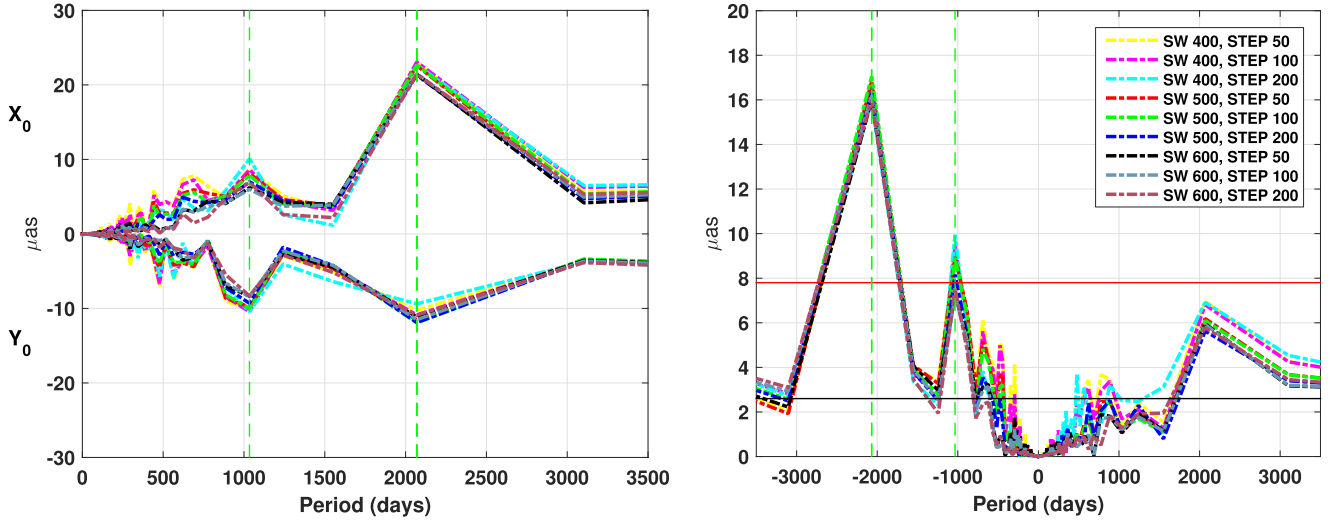
Figure 6. Fourier spectra of the parameters X_0 and Y_0(left), and $X_0 + i Y_0$ (right), estimated along with the FCN, with different window lengths and step sizes. The 1σ and 3σ confidence levels are displayed as horizontal black and red lines, respectively. Green vertical lines are inserted at the periods that exhibit significant signals: 1034 and 2069 days.
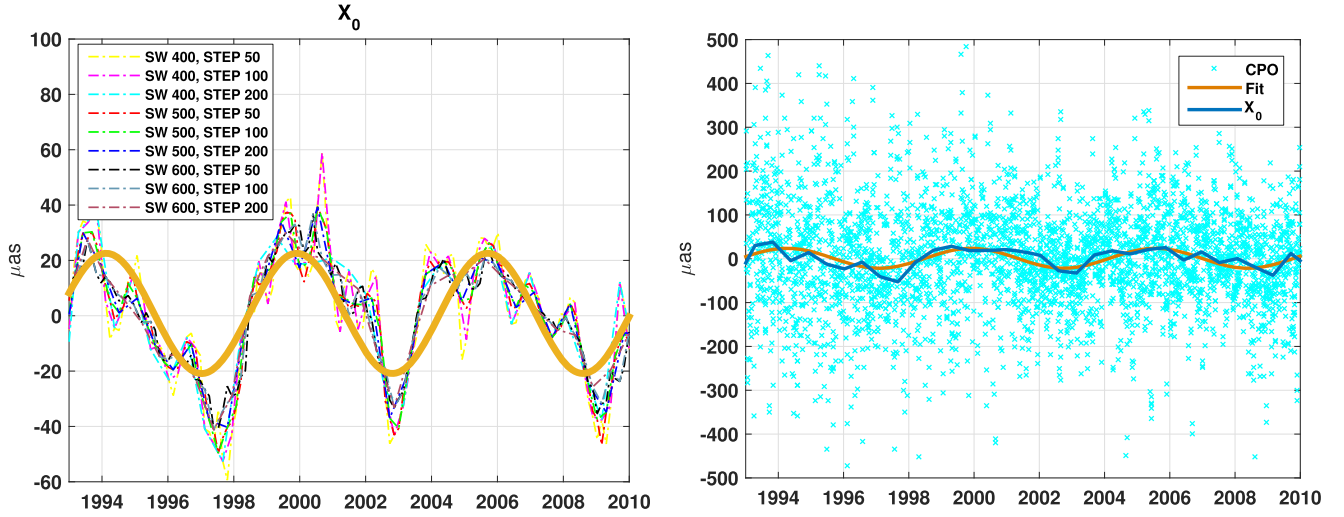

Figure 7. Left: constant offsets X_0 estimated using Equation (4), with different sliding window lengths and step sizes. Right: fit of the precession constant X_0 based on the residuals after the fit of the main nutation amplitudes and the FCN amplitudes.
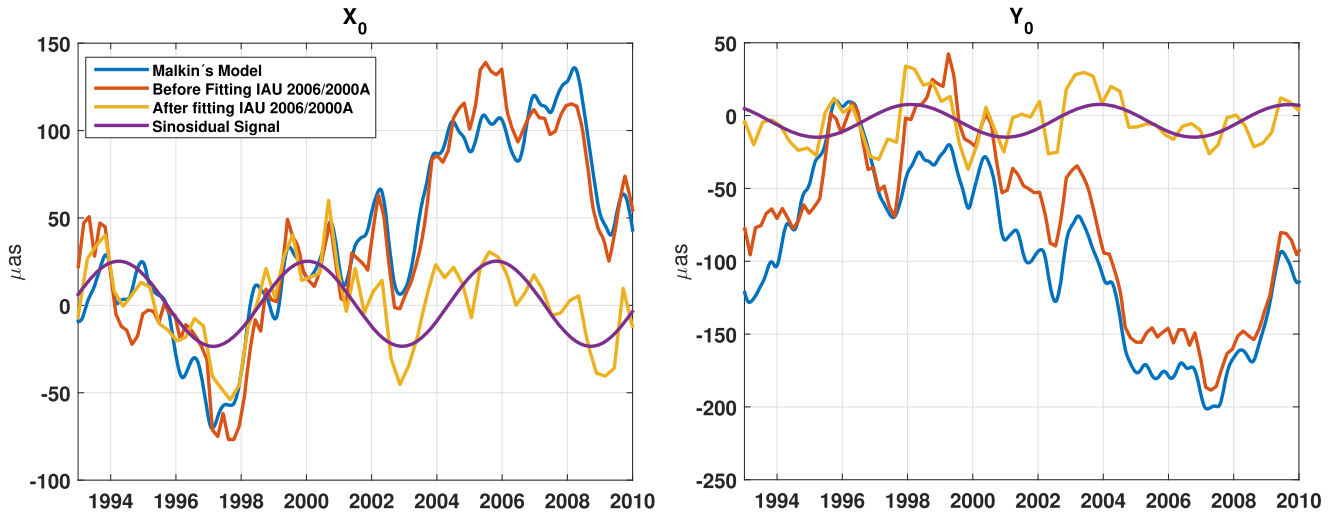
Figure 8. Comparison of the offsets X_0 and Y_0 estimated in this study, provided by Malkin (2013a) (http://www.gao.spb.ru/english/as/persac/), and based on the residuals after empirical correction of the main nutation amplitudes and the FCN amplitudes using a sliding window length of 400 days and a step size of 100 days.
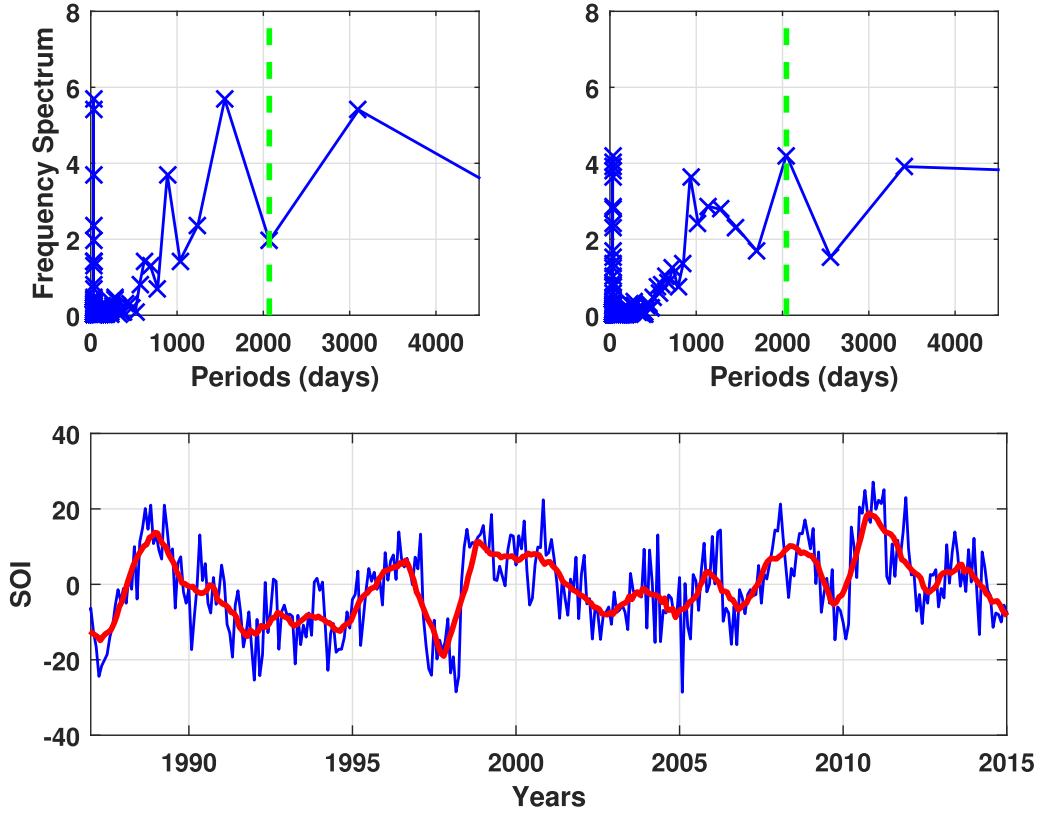
Figure 9. SOI (bottom) and its Fourier spectra considering different periods: 1993 to 2010, corresponding to the time span of the VLBI data (left), and 1987 to 2015 (right).
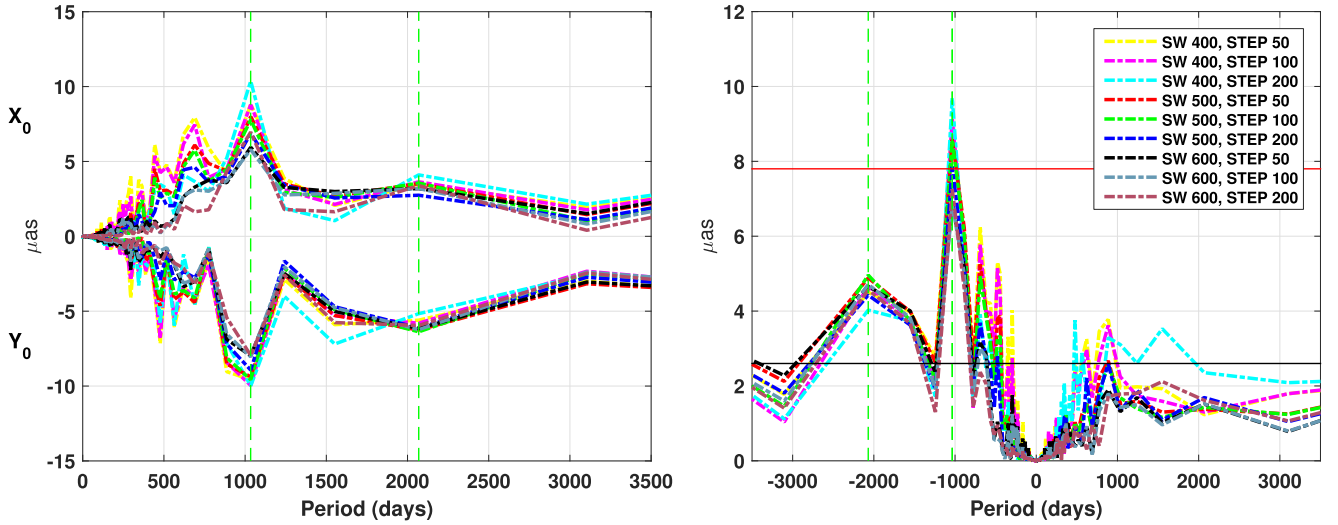

Figure 10. Fourier spectra of the offsets X_0 and Y_0(left), and $X_0 + i\, Y_0$ (right) estimated using Equation (4) after removing the 2069-day signal, for a selection of different window lengths and step sizes. The 1σ and 3σ confidence levels are displayed as horizontal black and red lines, respectively. Green vertical lines are inserted at the periods of 1034 days and 2069 days discussed in the text.

can be easily identified in the remaining residuals, predominantly in the X component. While adopting a fixed value for the FCN period, its time-variable amplitudes and phases were estimated based on various sliding window lengths (400, 500, and 600 days) displaced by different step sizes (50, 100, and 200 days). This test allows us to assess possible impacts due to the assumption of certain numerical values avoiding misleading conclusions caused by possible hidden mathematical artifacts. As can be seen in the Fourier spectra (Figure 6) and the X_0 parameter

(Figure 7), essentially the same behavior and peaks at 2069 days were obtained when using different window lengths and step sizes. This indicates that this predominant retrograde signal is of physical nature.

Next, X_0 and Y_0, the window-dependent constant offsets estimated before fitting the amplitudes of the main nutation terms of the IAU 2006/2000A model, were compared to the similar parameters determined by Malkin (2013a), which were computed using 430 day long groups of data and a step size of
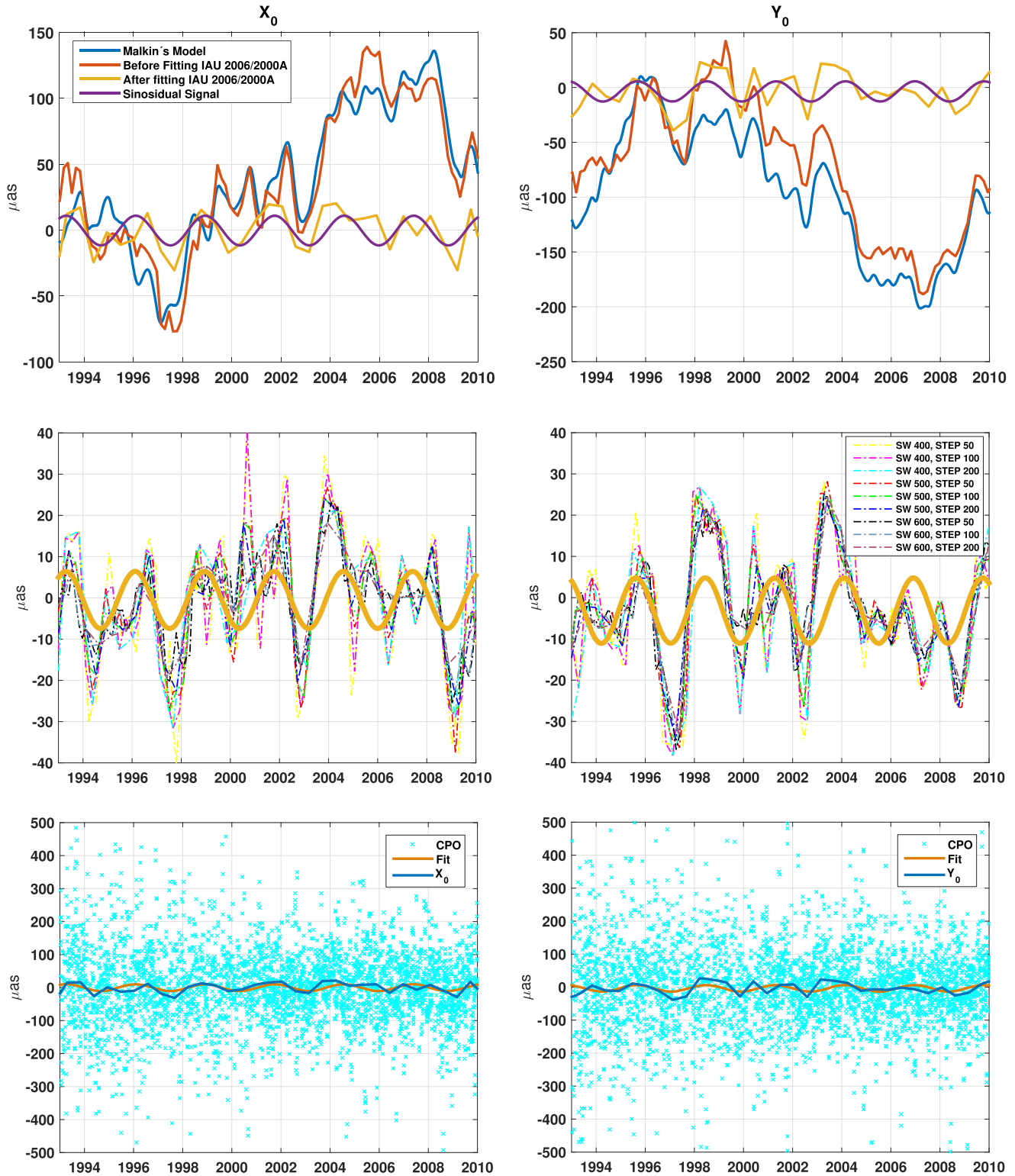
Figure 11. Upper row: comparison of the offsets X_0 and Y_0 estimated in this study in comparison to the values provided by Malkin (2013a) (http://www.gao.spb.ru/english/as/persac/), as well as the fit of X_0 and Y_0 based on the residuals after empirical correction of the main nutation amplitudes and the FCN amplitudes using a sliding window length of 400 days and a step size of 100 days. Middle: offsets (X_0, Y_0) estimated using the FCN equations with different window width strategies shown in the legend. Bottom: fit of the offsets using the remaining residuals. Left: X component, right: Y component.

1 day. The results for Malkin's solution and ours with a window length of 400 days and advancing each 100 days, are shown in Figure 8. The two curves have a similar shape, which indicates positive validation of our new solution. A third solution is displayed in the figure that was obtained as follows:

the signal composed by the corrections to the IAU2000 amplitudes is subtracted from the residuals and then the FCN time-varying amplitude is re-fitted too, again by means of a sliding window method with a 400-day window length and a 100-day step forward, which provides a new time series (X_0, Y_0)
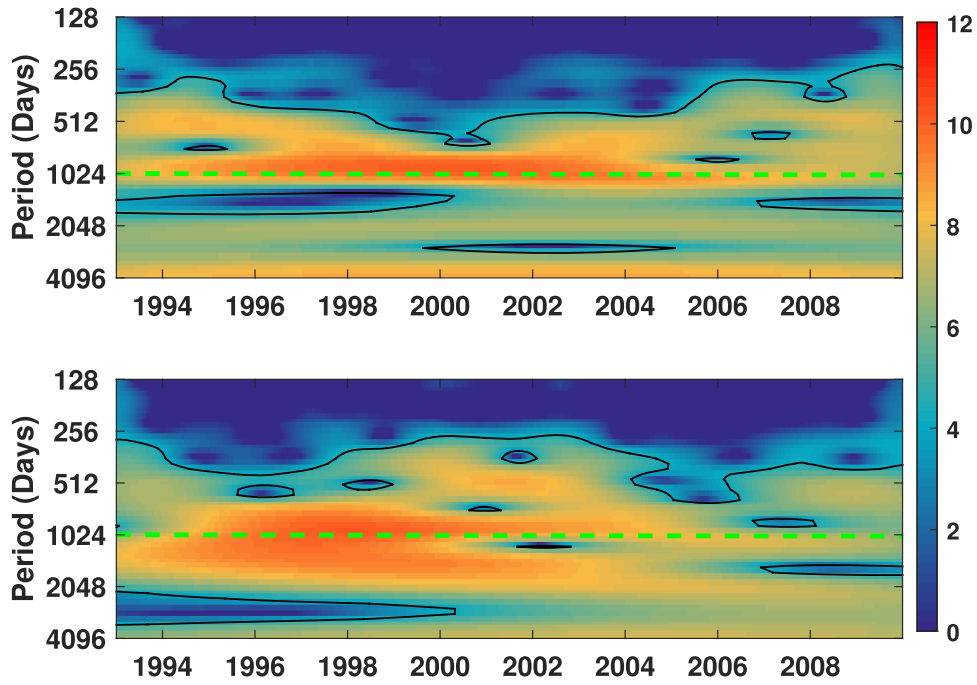
Figure 12. Morlet–Wavelet energy spectrum of the constant offsets X_0 (top) and Y_0 (bottom) estimated using Equation (4). The x-axis shows the time domain (years) and the y-axis shows the frequency domain as given in periods (days). Constant offsets are estimated with a sliding window length of 400 days and a step size of 100 days. The green horizontal dashed lines denote the period of 1035 days where the FICN is expected (Mathews et al. 2002). Approach A1. Units: power.
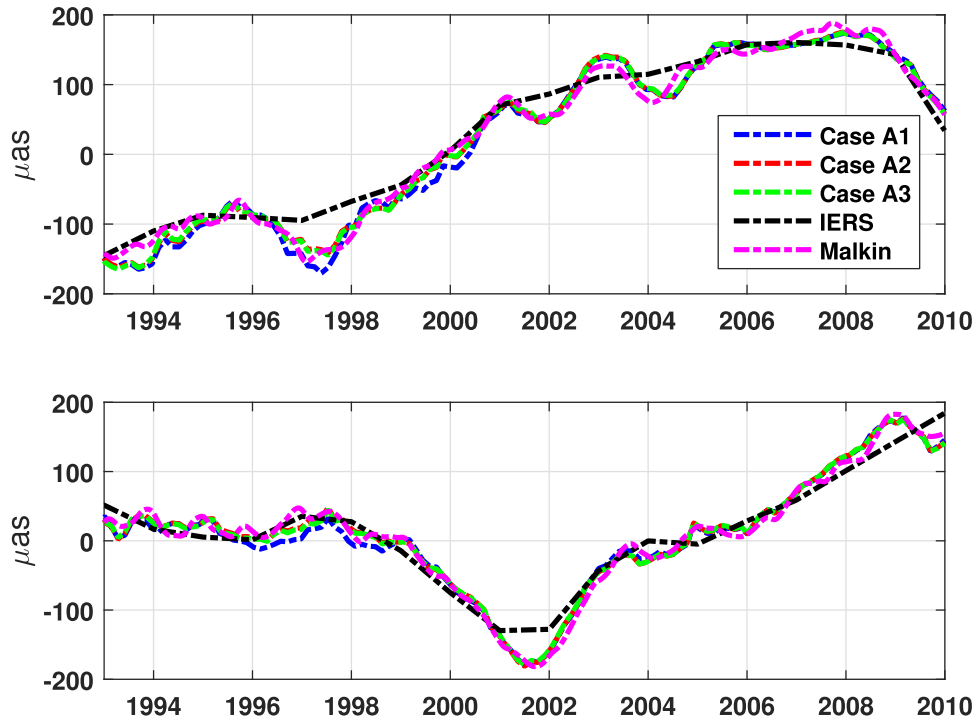

Figure 13. Coefficients A_c (top) and A_s (bottom) of different empirical FCN models computed with a sliding window length of 400 days and a step size of 50 days using USNO finals as a priori EOPs, along with the values published in the IERS Conventions (2010) and the coefficients estimated by Malkin (2013a), during the interval 1990–2010.

showing less variability than the other two. The sinusoidal signal is superimposed on the third solution and looks to be quite in agreement with it (left plot).

That apparent signal with a period of about 5.7 yr shows amplitudes of about 25 μas and 10 μas in X and Y, respectively,

which could be taken into consideration for future improvements and could be attributed to a variety of potential candidates that share similar periodicity. It could be caused/ mimicked by, e.g., (1) strong ENSO (El-Nino Southern Oscillation) events; (2) geomagnetic jerk (GMJ) events as

Table 4
Solution Difference Statistics/Statistical Analysis of the Residuals

| A Priori Values | | Before re-fitting | | After re-fitting | | Removing Signals | | Removing | |
| | | IAU 2006/2000A | | IAU 2006/2000A | | 5.7 years/2.8 years | | FCN Model | |
TRF	EOP	r_x	r_y	r_x	r_y	r_x	r_y	r_x	r_y
	USNO finals								
ITRF2014	CPO	183.5	196.2	170.5	179.9	169.5	179.6	133.1	146.7
	IAU 2006/2000A	175.4	180.7	162.8	164.9	161.7	164.6	124.3	128.2
	IAU 2006/2000A + FCN	174.2	180.2	161.9	164.3	160.7	164.0	123.2	127.8
	IERS 08 C04								
ITRF2014	CPO	196.8	200.1	181.9	183.8	181.3	183.5	148.5	152.6
	IAU 2006/2000A	175.2	179.7	162.7	164.0	161.6	163.7	123.6	127.7
	IAU 2006/2000A + FCN	174.5	179.0	162.6	163.9	161.5	163.6	123.5	127.6
	USNO finals								
ITRF2008	CPO	179.7	194.4	167.0	177.9	165.9	177.6	129.0	144.3
VTRF2008	CPO	180.1	194.6	167.5	178.1	166.4	177.8	129.7	144.4

Note. Comparison of root mean squares r of the residuals before and after fitting the main nutation amplitudes of the IAU 2006/2000A precession-nutation models, considering observed periodic signals of about 2.8 yr and 5.7 yr, plus the FCN. Units: μas.

pointed out by Malkin (2013a) and Shirai et al. (2005); (3) errors in the nearby 2120.652 day nutation term determination; (4) a modulation phenomenon associated with the proximity of the FCN and nearly annual frequencies (see, e.g., Gattano et al. 2016); or (5) the 5.8 ± 0.8 yr oscillation present in the length of day (LOD) attributed to gravitational coupling between the mantle and inner core (Mound & Buffet 2006), among other potential factors. The investigation of the origin of that signal is out of the scope of our paper, which focuses on improving CPO modeling with an empirical approach. Nevertheless, the ENSO possibility (1) was roughly investigated by performing a spectral analysis of the time series representative of the Southern Oscillation index—SOI (Figure 9). The results were not conclusive since they lack robustness: analyzing the period 1993–2010, the highest spectral peak is located around 1500 days, but extending the time span from 1987 to 2015 the maximum power moves to the neighborhood of 2000 days.

After pre-whitening the residuals from the 5.7 yr signal, the remaining residuals were again reexamined using the offsets X_0 and Y_0- determined from Equation (4). Now, the harmonic constituent with maximal amplitude is exactly located at 1034 days (2.8 years) for both X and Y components in all the tested scenarios (Figure 10, left). That period is almost equal to the 1035 ± 52 days that Mathews et al. (2002) assigned to the FICN in the celestial frame.[5] The possibility of associating the detected 1034-day periodic term to the FICN was assessed by means of Fourier analysis estimated from the complex quantity $X_0 + iY_0$. The obtained Fourier spectra (Figure 10, right) provide clear evidence of a signal in the retrograde nutation frequency band (negative period) at about 1034 days.

Figure 11 is similar to Figure 8, but the third solution has been changed by a new one derived from the residuals after cleaning the 5.7-yr oscillation. It can be seen in the upper plots of Figure 11 that the slow variation patterns of X_0 and Y_0 associated with the 18.6-yr and 5.7 yr periods have disappeared after applying the empirical corrections derived so far in the

paper. The periodic signal near 1034 days that was mentioned before is now dominant and can be easily identified and recognized in the time series offsets (Figure 11, upper row); this signal is implicit in the remaining residuals (Figure 11, bottom row) and the robustness of its determination is illustrated in (Figure 11, middle row). In order to study the temporal variation of this signal, we determined the distribution of energy within the data by using a Morlet–Wavelet power spectrum (Figure 12).

The wavelet analysis (Figure 12) reveals a temporally relatively stable oscillation with a period of about 1034 days at the level of about 10 μas, especially in the X component between 1993 and 2010, and in the Y component between 1995 and 2006. The strong energy distribution is less clear and smaller in the Y component in early and late years, which is probably caused by an aliasing effect with other frequencies (e.g., 1500 days), but wavelet scalograms should not be seriously interpreted at the data borders due to possible edge effects. These pictures are similar for all the analyzed series in this study and for all the various approaches (Figure 11, middle). Therefore, the same conclusions can be drawn when using different sliding window lengths and step sizes for the fits.

Finally, in Figure 13 we show a comparison of the different estimated empirical FCN models using different a priori CPO coordinates (cases A1, A2, and A3) w.r.t. current models (IERS, i.e., Lambert 2007, and Malkin 2013a) in order to ensure the consistency of our results and the followed methodology during the study. Note that all the amplitudes A_c and A_s are reasonably close to each other along the whole period.

5. Conclusions

In this paper, we obtain corrections to the precession offsets and rates, and to the amplitudes of a wide set of terms of the IAU 2006/2000A precession-nutation model. These corrections are derived from several solutions of the celestial pole coordinates determined from a global analysis of VLBI sessions in the period 1990–2010 applying different a priori data, such as EOPs and TRFs. We find that the tested TRFs do not have a considerable influence on the CPO estimates in our approach. However, using

---

[5] As pointed out by the cited study, that period is retrograde-diurnal w.r.t the terrestrial frame and prograde long-periodic w.r.t the celestial frame.

different a priori CPO results in slight deviations, particularly to the precession rate and the scatter of the residuals. The error analyses, displayed in Tables 2 and 4, show that the most accurate results (minimum rms) are always obtained when including the IAU 2006/2000A model plus the FCN model published by Belda et al. (2016) as a priori CPC (case A3).

Including the VLBI sessions after 2010 leads to increasingly different precession rate estimates. The reason is not obvious; although a plausible explanation could be that the ICRF2 is only fully consistent with data before 2009 March. After this date, the nutation estimates by VLBI could absorb the limitations of the CRF. This means that the ICRF2 needs to be updated as already done for the current conventional EOP series and TRF, in order to improve the consistency with the more recent VLBI data. A new release, "ICRF3," is expected to be presented at the upcoming IAU General Assembly in 2018.

A statistical analysis of the residuals (Table 4) between the reported time series (approaches A and B) before and after re-fitting the main nutation terms demonstrates that the empirical corrections (Table 3) attain an error reduction by almost 15 μas ($\approx$0.5 millimeters) for both the X and Y components. Furthermore, using the most consistent VLBI data w.r.t ICRF2 revealed two apparent predominant retrograde signals, one at about 2069 days and one at about 1034 days, the former being clearly statistically significant. Considering these long-term periodic signals results in a modest mean improvement of about 1 μas and 0.3 μas in the X and Y directions, respectively, as can be seen by comparing the pairs of columns 5/7 and 6/8 in Table 4. Finally, the rms of the residuals after FCN amplitudes have been removed show mean values close to 130 μas (Table 4).

For further improvement of the estimates in the future, we think that the following points should be addressed, among others: (i) put more stringent constraints on the theoretical estimates; (ii) identify inconsistencies between TRFs and CRFs; (iii) consider further unmodeled geophysical signals; (iv) update the ICRF2 in terms of consistency with the involved TRF; and (v) combine different space geodetic techniques (i.e., VLBI and LLR).

ORCID iDs

Santiago Belda ⓘ https://orcid.org/0000-0003-3739-6056

References

Altamimi, Z., Collilieux, X., & Metivier, L. 2011, JGeod, 85, 457
Altamimi, Z., Rebischung, P., Métivier, L., & Collilieux, X. 2016, JGRB, 121, 6109
Belda, S., Ferrándiz, J.-M., Heinkelmann, R., Nilsson, T., & Schuh, H. 2016, JGeo, 94, 59
Belda, S., Ferrándiz, J. M., Heinkelmann, R., Nilsson, T., & Schuh, H. 2017, JGeod, 91, 135
Bizouard, C., & Gambis, D. 2009, in International Association of Geodesy Symp. 134, The Combined Solution C04 for Earth Orientation Parameters Consistent with International Terrestrial Reference Frame 2005, ed. H. Drewes (Berlin: Springer), 265, doi:10.1007/978-3-642-00860-3_41
Böckmann, S., Artz, T., & Nothnagel, A. 2010, JGeod, 84, 201
Böhm, J., Böhm, S., Nilsson, T., et al. 2012, in International Association of Geodesy Symposia 136, Geodesy for Planet Earth, ed. S. Kenyon, M. Pacino, & U. Marti (Berlin, Buenos Aires: Springer), 1007, doi:10.1007/978-3-642-20338-1_126
Capitaine, N., Mathews, P., Dehant, V., Wallace, P., & Lambert, S. 2009, CeMDA, 103, 179
Capitaine, N., Wallace, P. T., & Chapront, J. 2003, A&A, 412, 567
Capitaine, N., Wallace, P. T., & Chapront, J. 2005, A&A, 432, 355
Chao, B., & Hsieh, Y. 2015, E&PSL, 432, 483
Charlot, P., Sovers, O. J., Williams, J. G., & Newhall, X. X. 1995, AJ, 109, 418
Dehant, V., de Viron, O., & Greff-Lefftz, M. 2005, A&A, 438, 1149
Dehant, V., Feissel-Vernier, M., de Viron, O., et al. 2003, JGRB, 108, 2275
Fey, A. L., Gordon, D., Jacobs, C. S., et al. 2015, AJ, 150, 58
Gattano, C., Bizouard, C., & Lambert, S. 2016, in International VLBI Service for Geodesy and Astrometry, The Annual Retrograde Nutation Variability, ed. D. Behrend et al., 341, NASA/CP-2016-219016
Gattano, C., Lambert, S., & Bizouard, C. 2017, JGeod, 91, 849
Haas, R. 2004, in Proc. 7th European VLBI Network Symp., Analysis strategies and software for geodetic VLBI, ed. R. Bachiller et al. (Toledo: Observatorio Astronómico Nacional), 297
Herring, T., Mathews, P., & Buffet, B. 2002, JGRB, 107, 2069
Krásná, H., Böhm, J., & Schuh, H. 2013, A&A, 555, A29
Lambert, S. 2007, Empirical Modeling of the Retrograde Free Core Nutation. Technical Note, ftp://hpiers.obspm.fr/iers/models/fcn/notice.pdf
Lambert, S., & Dehant, V. 2007, A&A, 469, 777
Liu, J. C., & Capitaine, N. 2017, A&A, 597, A83
Malkin, Z. 2013a, JGeo, 72, 53
Malkin, Z. 2013b, in Proc. Journees 2013 Systemes de Reference Spatio-temporels, On detection of the free inner core nutation from VLBI data, ed. N. Capitaine (Paris), 224
Mathews, P. M., Buffett, A., Herring, T. A., & Shapiro, I. I. 1991, JGRB, 96, 8219
Mathews, P. M., Herring, T. A., & Buffett, B. A. 2002, JGRB, 107, 2068
Mound, J. E., & Buffet, B. A. 2006, E&PSL, 243, 383
Nilsson, T., Soja, B., Karbon, M., Heinkelmann, R., & Schuh, H. 2015, EP&S, 67, 136
Nothnagel, A., Alef, W., Amagai, J., et al. 2015, The IVS data input to ITRF2014 in GFZ Data Services, Helmholtz Centre, Potsdam, Germany, doi:10.5880/GFZ.1.1.2015.002
Petit, G., & Luzum, B. 2010, IERS Technical Note 36, 179 (Verlag des Bundesamts für Kartographie und Geodäsie; Frankfurt am Main) (https://www.iers.org/IERS/EN/Publications/TechnicalNotes/tn36.html)
Petrov, L. 2007, A&A, 467, 359
Plag, H., & Pearlman, M. 2009, Global Geodetic Observing System: Meeting the Requirements of a 20 Global Society on a Changing Planet in 2020 (Berlin: Springer)
Seidelmann, P. K. 1982, CeMec, 27, 79
Shirai, T., Fukushima, T., & Malkin, Z. 2005, EP&S, 57, 151
Smith, M. 1977, GeoJI, 50, 103
Toomre, A. 1974, GeoJI, 38, 335
Urban, S. E., & Seidelman, P. K. 2013, Explanatory Supplement to the Astronomical Almanac for the Year 2013 (3rd ed.; Mill Valley, CA: Univ. Science Books)
Wahr, J. 1981, GeoJI, 64, 705